International Journal of Pharmaceutics 419 (2011) 314–321

Contents lists available at ScienceDirect

International Journal of Pharmaceutics

journal homepage: www.elsevier.com/locate/ijpharm

Pharmaceutical Nanotechnology

Structure and remodeling behavior of drug-loaded high density lipoproteins and their atherosclerotic plaque targeting mechanism in foam cell model

Wen-Li Zhang[a], Yan Xiao[a], Jian-Ping Liu[a,*], Zi-Mei Wu[b,**], Xiao Gu[a], Yi-Ming Xu[c], Hui Lu[c]

[a] Department of Pharmaceutics, China Pharmaceutical University, Nanjing 210009, PR China
[b] School of Pharmacy, University of Auckland, Private Bag 92019, Auckland, New Zealand
[c] Atherosclerosis Research Centre, Nanjing Medical University, Nanjing 210029, PR China

ARTICLE INFO

Article history:
Received 19 April 2011
Received in revised form 25 July 2011
Accepted 26 July 2011
Available online 30 July 2011

Keywords:
Reconstituted high density lipoproteins
Discoidal rHDL
Spherical rHDL
Foam cells
Atherosclerotic plaque targeting

ABSTRACT

This study is one of the first to test the relationship of formulation and structure of reconstituted high density lipoproteins (rHDL), drug behavior involved in remolding process and their targeting mechanism in a foam cell model. Tanshinone IIA-loaded rHDL (TA-rHDL) with different formulations and techniques were prepared and characterized. The targeting mechanism and drug behavior involved in remolding process were undertaken using a foam cell model. TA-rHDL prepared with cholesteryl ester (CE) and glycerol trioleate (TG) were spheres, or else discs. Guanidine hydrochloride denaturation experiments showed increased stability with TA-rHDL, compared to free apos. Phagocytosis tests demonstrated that the spherical TA-rHDL had targeting effect for foam cells through the scavenger receptor-BI and CE-TG interchange with TG-rich lipoproteins pathway under cholesteryl ester transfer protein. Discoidal TA-rHDL could reconstruct to spheres and target via a similar route as TA-rHDL spheres, showing a higher targeting efficiency. Lipophilic Tanshinone IIA could be re-entrapped in rHDL after remolding from discs to spheres and uptaken more by foam cells. Discoidal rHDL may serve as potential nanocarriers for targeting lipophilic cardiovascular drugs to atherosclerosis plaque.

1. Introduction

It has been well established that high-density lipoproteins (HDL) play a protective role against the development of cardiovascular diseases (Linsel-Nitschke and Tall, 2005) due to their anti-atherogenic and anti-inflammatory properties (Barter et al., 2004). Reverse cholesterol transport (RCT) is considered as the key protective mechanism of HDL toward atherosclerosis. During RCT process, HDL particles enable excess cholesterol from extra-hepatic or peripheral tissues to be transported within the water-based bloodstream back to the liver for re-utilization or elimination through the biliary system (Lusis, 2000; Viles-Gonzalez et al., 2003). In healthy individuals, about thirty percent of blood cholesterol is carried by HDL.

Natural HDL have a Stoke's diameter of 5–17 nm (Assmann and Nofer, 2003) and exist in two different forms: one is nascent in discoidal shape, the other is mature in spherical shape. The former consists of apos, phospholipid bilayer and little cholesterol. The latter has a hydrophobic core of triglycerides (TG) and cholesterol esters (CE) covered with a monolayer of phospholipids in which apolipoprotein (apos) are embedded (Ajees et al., 2006; Libby et al., 2008; Thomas et al., 2008). The most abundant apo in HDL is apoA-I, a highly α-helical, 28.3 kDa polypeptide, taking up approximately 70% of the HDL protein mass (Vaisar et al., 2007). ApoA-I promotes cellular cholesterol efflux, binds lipids, activates lecithin:cholesterol acyl transferase (LCAT), and interacts with specific receptors, together with other apos such as apoA-II and apoE, plays a principal active role in HDL-therapy of coronary artery disease (Saito et al., 2004; Song et al., 2009). Acting in conjunction with LCAT which converts free cholesterol to cholesteryl ester, modulated by many factors, nascent discoidal HDL are converted and yield spherical HDL through remodeling the internal structure (Pownall and Gotto, 1992).

In the past decades, reconstituted HDL (rHDL) have been investigated as a delivery vehicle for many lipophilic drugs (Lou et al., 2005; McConathy et al., 2008; Oda et al., 2006) due to their attractive attributes. It was reported (Feng et al., 2008a,b; Lou et al., 2005)

Abbreviations: rHDL, reconstituted high density lipoproteins; TA-rHDL, Tanshinone IIA-loaded reconstituted high density lipoproteins; CE, cholesterol esters; TG, triglycerides; RCT, reverse cholesterol transportation; Apo, apolipoprotein; LCAT, lecithin:cholesterol acyl transferase; SR-BI, scavenger receptor-BI; TA, Tanshinone IIA; DLS, dynamic light scattering; EE, entrapment efficiency; TEM, transmission electron microscopy; GdnHCl, guanidine hydrochloride; ox-LDL, oxidized low density lipoproteins; CETP, cholesteryl ester transfer protein; VLDL, very low density lipoproteins.

* Corresponding author. Tel.: +86 25 83271293; fax: +86 25 83271293.
** Corresponding author. Tel.: +64 09 923 1709; fax: +64 09 367 7192.
E-mail addresses: liujianpingljp@hotmail.com (J.-P. Liu), z.wu@auckland.ac.nz (Z.-M. Wu).

0378-5173/$ – see front matter © 2011 Elsevier B.V. All rights reserved.
doi:10.1016/j.ijpharm.2011.07.039

that the central components of spherical rHDL can be replaced by hydrophobic drugs, while still maintaining the globular shape. On the other hand, the drug may be also entrapped in the phospholipid bilayer of the rHDL, forming liposome-like or discoidal structure. In addition, the discoidal rHDL administered systemically have high affinity with LCAT, resulting in subsequent remodeling of the rHDL from the discoidal form to the spherical like the natural HDL (Nanjee et al., 1999). However, up to date there are no reports available investigating the exact structures of drug loaded rHDL with different compositions or the drug behavior during rHDL conversion. This conversion is envisioned to cause the drug leak out or re-entrapped into lipid cores of the remodeled spherical rHDL, resulting in different fates *in vivo*.

Recently, there are growing evidences showing the potential of targeting effect of drug-free rHDL for atherosclerosis plaque. Skajaa et al. (2010) have found that iron oxide core-HDL particles were able to circulate as single entities and enter the plaque sites individually, in a similar manner as native HDL *in vivo*. One possible mechanism of rHDL for other targeting tissues is considered to be associated with direct targeting of apoA-I to the ABCA1 protein, ABCG-I and scavenger receptor-BI (SR-BI) receptors on the foam cells in the arteries (Collet et al., 1999; Fitzgerald et al., 2010; Zannis et al., 2006). While given the consideration of lipids transfer between HDL and different lipoproteins (Skajaa et al., 2010), the other mechanism may be similar to the indirect targeting effect (Collet et al., 1999) realized by other TG-rich lipoproteins (e.g. very low density lipoproteins) in the blood. Atherosclerotic lesions are characteristic of many lipid-laden "foam cells" (Bobryshev, 2006), which are derived from the monocytes that invade the intima of lesion-prone areas in arteries and consequently become phagocytic and accumulate lipid. So far, the mechanisms by which the rHDL target atherosclerosis plaque have not been defined, neither have drug-loaded rHDL.

The present study was to develop a drug-loaded rHDL system with dual roles of targeting the drug to atherosclerosis plaque and simultaneously providing therapeutic effect of the carrier. Tanshinone IIA (TA), a well-known traditional Chinese medicine for treating atherosclerosis, was selected as a model drug. In the previous study from the laboratory (Zhang et al., 2010), TA-NLC (Tanshinone IIA loaded nanostructured lipid carriers) was reconstituted only with lipid components of native HDL, which could compete for apos of native HDL *in vitro*. However, formulations with the apos and their targeting potential or bionic function were not considered. In this study, TA-loaded rHDL (TA-rHDL) with different structures have been constituted and characterized from the standpoint of a new drug delivery system including the particle size, entrapment efficiency, structure, and the apos–lipid interactions. Specially, TA-rHDL with magnified size served as a tentative model of native HDL to allow visualization of its structure and remodeling behavior. The study also aimed to explore the targeting potential of TA-rHDL as well as the mechanisms and structure factors involved using an *in vitro* foam cell model mimicking the atherosclerosis plaque.

2. Materials and methods

2.1. Materials

Tanshinone IIA (98% pure) was purchased from Xi'an honson biotechnology Co., Ltd. (China). Lipoid S 100 was obtained from Lipoid GmbH (Germany). Cholesterol and cholesteryl oleate was purchased from Sigma–Aldrich chemie GmbH and Alfa Aescar/Johnson matthey Co., Ltd., respectively. Glycerol trioleate was product of Tokyo Kasei Kogyo Co., Ltd. (Japan). The whole apos (97% pure) in HDL with 59% as apoA-I were isolated from the industrial waste during production of albumin in our laboratory. Sephadex G50 was purchased from Pharmacia (Sweden). Human plasma was supplied by Nanjing Red Cross. RAW 264.7 cells were obtained from American Type Culture Collection. Native HDL and very low density lipoproteins were prepared by ultracentrifugation in our laboratory. Oxidized low density lipoproteins of human were purchased from Yuanyuan Biotechnology (Guangzhou, China). Lipid-free BSA (A2000) was supplied by APPLYGEN Technologies (Beijing, China). Pancrelipase were obtained from Sigma–Aldrich (L3126). β-Mercaptoethanol were purchased from Sigma–Aldrich. All other reagents used in this study were of analytical grade except methanol of chromatographic grade.

2.2. Preparation of drug-loaded spherical and discoidal rHDL

The preparation process consisted of construction of the lipid cores and subsequent formation of TA-rHDL by incubation of the lipid cores with apos. Formulations of lipid cores as nanoparticles or liposomes were prepared with or without cholesteryl oleate (CE) and glycerol trioleate (TG) using the following techniques.

The lipid cores of TA-rHDL were prepared by a nanoprecipitation/solvent diffusion method as previously described (Zhang et al., 2010) with (named as cores of TA-rHDL$_a$) or without (named as cores of TA-rHDL$_b$) CE and TG except that sodium cholate was added in the water phase to mediate later coupling with proteins. Briefly, Tanshinone IIA, TG, cholesterol with or without CE were dissolved in acetone (8 mL) by sonication (DL-720, Shanghai, China), then soybean lecithin dissolved in 2 mL of absolute ethanol was added to acetone to form an organic phase maintained at 60 ± 2 °C. Then the organic phase was injected slowly into an aqueous phase of the same temperature, which contains 0.1 M KC1, 1 mM EDTA and 0.01 M Tris–HCl, pH 8.0 in double distilled water (30 mL). Then a semi-transparent pre-emulsion was obtained under constant magnetic agitation. After ultrasonication for 200 s using Ultrahomogenizer (JY 92II, Ningbo, China), the dispersion was transferred to a rotary evaporator to remove organic solvent at 65 °C under reduced pressure. The prepared lipid cores of TA-rHDL were filtered through 0.22 μm filters after cooling down to room temperature.

Thin-film dispersion method was alternatively employed to prepare the cores of TA-rHDL without CE and TG (named as cores of TA-rHDL$_c$). Briefly, TA, soy lecithin, cholesterol and sodium cholate were dissolved in dehydrated alcohol and dried in an eggplant-shaped flask. 0.01 M Tris buffer (0.1 M KC1, 1 mM EDTA, pH 8.0) was added, then the mixture was vortexed thoroughly for 5 min, followed by ultrasonication for 300 s using an Ultrahomogenizer (JY 92II, Ningbo, China) until a clear suspension was obtained. The dispersion was then filtered through 0.22 μm filters to remove larger particles and the filtrate was dialyzed to remove the free sodium cholate using dialysis bags (MW cut off 14,000 Da).

The lipid particles obtained above were incubated with the apos to form TA-rHDL. A preliminary study was performed to determine the optimal conditions in order to achieve the highest apo coupling efficiency for TA-rHDL. Ultimately, 2 mL of cores of TA-rHDL$_a$ were incubated with 14 mg apos under 600 rpm stirring at 37 °C for 8 h. Cores of TA-rHDL$_b$ or T-rHDL$_c$ were incubated at low temperature instead (4 °C) to ensure their intact structures.

2.3. Size, Zeta potential and drug entrapment efficiency

Size and Zeta potential of TA-rHDL$_a$, TA-rHDL$_b$ and TA-rHDL$_c$ were measured with dynamic light scattering (DLS) using a Zetasizer 3000 HSA (Malvern, UK). Samples were diluted appropriately with aqueous phase prior to the measurements.

Drug entrapment efficiency was determined using the mini-column centrifugation method (Fry et al., 1978; Jain et al., 2008).

Generally, to prepare the mini-columns, absorbent cotton was inserted in the bottom of the 5-mL plastic syringes which was then filled with swollen Sephadex G50. Then the column was inserted into a test tube. Excess water was removed by centrifugation at 2000 r/min for 6 s, and 400 μL of the TA-rHDL suspensions were added dropwise to the center of the column, followed by centrifugation at 1000 r/min for 5 min. Distilled water (400 μL) was added and centrifugation was applied to force the TA-rHDL through the column into the test tube while the free drug was retained in the Sephadex matrix. TA-rHDL particles were recovered from the first and second stages of centrifugation.

Secondly, concentrations of TA entrapped in the TA-rHDL (C) and the total drug in TA-rHDL suspension (C_0) were determined by HPLC, respectively, after dilution with absolute ethanol. Entrapment efficiency (EE) was calculated with the following formula:

$$\mathrm{EE}(\%) = \frac{C}{C_0} \times 100 \quad (1)$$

2.4. Visualization by transmission electron microscopy (TEM)

The TA-rHDL particles before (i.e. the lipid cores) and after incubation with apos were diluted appropriately with aqueous phase. A drop of each sample was applied to a copper grid coated with carbon film and air-dried; 2% (w/v) phosphotungstic acid (PTA) solution was then dropped onto the grids. After being negative stained and air-dried at room temperature, the samples were visualized by TEM (H-7650, Hitachi, Japan).

2.5. Structure certification of TA-rHDL lipid cores

Since calcein can only be entrapped in the aqueous cavities of liposomes but not in the lipophilic spheres, the internal structure feature of TA-rHDL and the change during conversion from lipid cores to rHDL can be revealed by the calcein content and its variation, respectively.

Calcein, an aqueous fluorescent marker, was dissolved in Tris buffer and used as aqueous phase during preparation of TA-rHDL. Then un-capsulated calcein was separated from the particles through a 5 mL minicolumn of Sephadex G50 by centrifugation as described in Section 2.3 and the concentrations were determined by fluorescence spectrophotometry (Shimadzu RF-5301PC). The contents of calcein in various TA-rHDL and their cores were subsequently determined to interpret the internal structures of TA-rHDL and the structural changes before and after incubation with apos.

2.6. Guanidine hydrochloride denaturation experiments

Guanidine hydrochloride (GdnHCl) solutions were prepared in the standard Tris buffer (pH 8.0) devoid of NaCl and was pre-warmed to 25 °C. 0.5 mL of apos alone or TA-rHDL particles with protein concentrations around 0.15 mg/mL, also pre-equilibrated to 25 °C, was added to the GdnHCl solution to give the stated GdnHCl concentration of 2 M. The first scan of fluorescence spectrum was started 30 s after mixing and completed within 2 min. The samples were kept at 25 °C and scanned again at 0.5, 1, 2, 4, 6, 10 and 24 h. The λ_{em} shift of fluorescence at each time point using 280 nm exciting light was recorded to observe the denaturation of apos.

2.7. Phagocytosis tests

Mouse macrophage cell line RAW264.7 and foam cell derived from macrophage were employed to study the mechanism of targeting and the relationship between structures of rHDL and phagocytosis.

2.7.1. Cell culture

Mouse macrophage cell line RAW 264.7 were routinely cultured in Dulbecco's Modified Eagle Medium (DMEM) (Sigma, St. Louis, USA) containing 10% fetal bovine serum with penicillin (100 U/mL) and streptomycin (100 pg/mL) at 37 °C in humidified, 5% CO_2, 95% air. The macrophage cells were seeded in 24-well tissue culture plates at 1×10^5 cells/well. To obtain foam cells, the macrophage cells were treated with 100 μg/mL oxidized low density lipoproteins (ox-LDL) for 24 h (Xie et al., 2009). Fluorescence microscopic examination of these macrophages revealed a significant accumulation of oil red O in the cells, indicative of lipid accumulation and formation of foam cells.

2.7.2. Plasmid amplification and foam cell transfection

Plasmid DNAs expressing human cholesteryl ester transfer protein (CETP) were amplified in DH-5α *Escherichia coli* and purified using a Genomic DNA kit (Tiangen Biotech). Then foam cells were transfected with plasmid using LipofectAMINE™ LTX reagent (Invitrogen, Carlsbad, CA). Twenty-four hours after the transfection, the cells expressing CETP were used for phagocytic uptake experiment.

2.7.3. Quantification of phagocytic uptake

In order to figure out the role of apos, both spherical TA-rHDL with and without apos (30 μg/mL, calculated by the TA content, 200 μL) were added to transfected foam cells expressing CETP and macrophages in the presence of lipid-free BSA (5 mg/mL) and β-mercaptoethanol (4 mM), respectively. To the foam cell model, very low density lipoproteins (VLDL, 2 mg/mL, 200 μL) were added as a giver of interchangeable lipids. At the meantime, CETP were added and followed by direct treatment by pancrelipase (80 mIU/mL). In another experiment, discoidal TA-rHDL were added to macrophages and transfected foam cells expressing CETP, respectively. In foam cell model, LCAT were investigated as a promoter for structure changes of discoidal TA-rHDL during phagocytosis. After an incubation periods of 1, 2 and 3 h, respectively, cells were washed three times with D-PBS to remove the non-phagocytosed drug. The washed cells were subject to five cycles of freezing (−40 °C) and thawing (37 °C) to split before dissolved in methanol (100 μL/well). The drug uptake was determined by analyzing the TA in the supernatant using HPLC as described previously (Zhang et al., 2010). The experiments were performed in triplicate.

2.7.4. Effects of LCAT by fluorescent microscopy

In order to confirm the morphological change of rHDL discs during cell incubation, fluorescently labeled rHDL discs were prepared by adding rhodamine 123 (100 μL) in absolute alcohol to the lipid phase or calcein (2 mg) in Tris buffer to the aqueous phase, respectively. The fluorescently labeled rHDL discs were obtained after the lipid cores were incubated with apos and the free fluorescent makers were removed using mini column centrifugation as described in Section 2.3.

The fluorescently labeled rHDL discs were added to foam cells expressing CETP in the presence or absence of LCAT and incubated for 1 h, 2 h and 3 h. VLDL and pancrelipase, essential to uptake, were added to the culture medium (DMEM). Then foam cells were washed and rinsed three times with D-PBS medium to remove the non-phagocytosed rHDL discs. The adhered cells phagocytozing labeled rHDL discs were visualized under a microscope equipped with epifluorescence optics (Nikon eclipse Ti-S, Japan).

Table 1
Average diameter, Zeta potential values, entrapment efficiency and drug loading (mean ± SD, $n = 3$) of TA-rHDL.

Formulation	Zeta potential (mV)		Size (nm)		EE%	Drug loading
	Before incubation	After incubation	Before incubation	After incubation		
TA-rHDL$_a$	−28.80 ± 0.15	−38.6 ± 0.10	58.4 ± 2.5	160.8 ± 5.6	97.8 ± 1.2	6.68 ± 0.02
TA-rHDL$_b$	−4.50 ± 0.08	−10.43 ± 0.15	60.2 ± 3.3	164.3 ± 5.3	82.6 ± 1.6	4.43 ± 0.05
TA-rHDL$_c$	−4.60 ± 0.04	−16.37 ± 0.12	63.8 ± 3.4	162.1 ± 6.8	91.3 ± 1.4	4.20 ± 0.15

2.8. Statistical analysis

Statistically significant differences were determined using two-tailed Student's *t*-test (SPSS, version 10.0). The *p* values for significance were set at 0.05 or 0.01.

3. Results

3.1. Size, Zeta potential and entrapment efficiency

Table 1 shows that the size of TA-rHDL$_a$, TA-rHDL$_b$ and TA-rHDL$_c$ were similar ($p > 0.05$) before (~60 nm) and after incubation with apos (~160 nm). However, the sizes of three formulations were all larger than that of the native HDL (5–17 nm). As expected, the coupling of apos also influenced the Zeta potential of the particles. The surface charge in TA-rHDL was all increased after incubation. And the surface charge in TA-rHDL$_a$ (−38.6 ± 0.10) was significantly more than that of native HDL (−12.4 ± 0.1).

3.2. Visualization by transmission electron microscopy

Morphology of TA-rHDL$_a$, TA-rHDL$_b$ and TA-rHDL$_c$ and their lipid cores was compared. As seen in Fig. 1, the increased size scale of three lipid cores after incubation coincided with the DLS data. Lipid cores of TA-rHDL$_a$ prepared with CE and TG were typical nanospheres and the spherical structure was still maintained after coupled with apos except that a brush shell was crowned. In comparison, the lipid cores of TA-rHDL$_b$ and TA-rHDL$_c$ prepared only with cholesterol and phospholipids with different techniques were both liposomes with a bilayer and vesicle structure. Interestingly, a dramatic structural change after coupling with apos from round vesicles to discoidal stacks was observed with both TA-rHDL$_b$ and TA-rHDL$_c$.

3.3. Structure certification of TA-rHDL lipid cores

As shown in Table 2, both TA-rHDL$_a$ and their lipid cores presented low fluorescence intensity, compared to TA-rHDL$_b$ and TA-rHDL$_c$. The fluorescence intensities of the calcein in TA-rHDL$_b$ and TA-rHDL$_c$ were 4–5 times higher than that of TA-rHDL$_a$. Moreover, there was no significant difference in fluorescence intensity between TA-rHDL$_a$ before and after incubation ($p > 0.05$). In contrast, leakage of calcein from TA-rHDL$_b$ (34%) particularly TA-rHDL$_c$ (48.8%) during incubation was observed. It was also notable that despite fluorescence intensity in the lipid cores of TA-rHDL$_c$ was higher than that of TA-rHDL$_b$, the loss of calcein from TA-rHDL$_c$

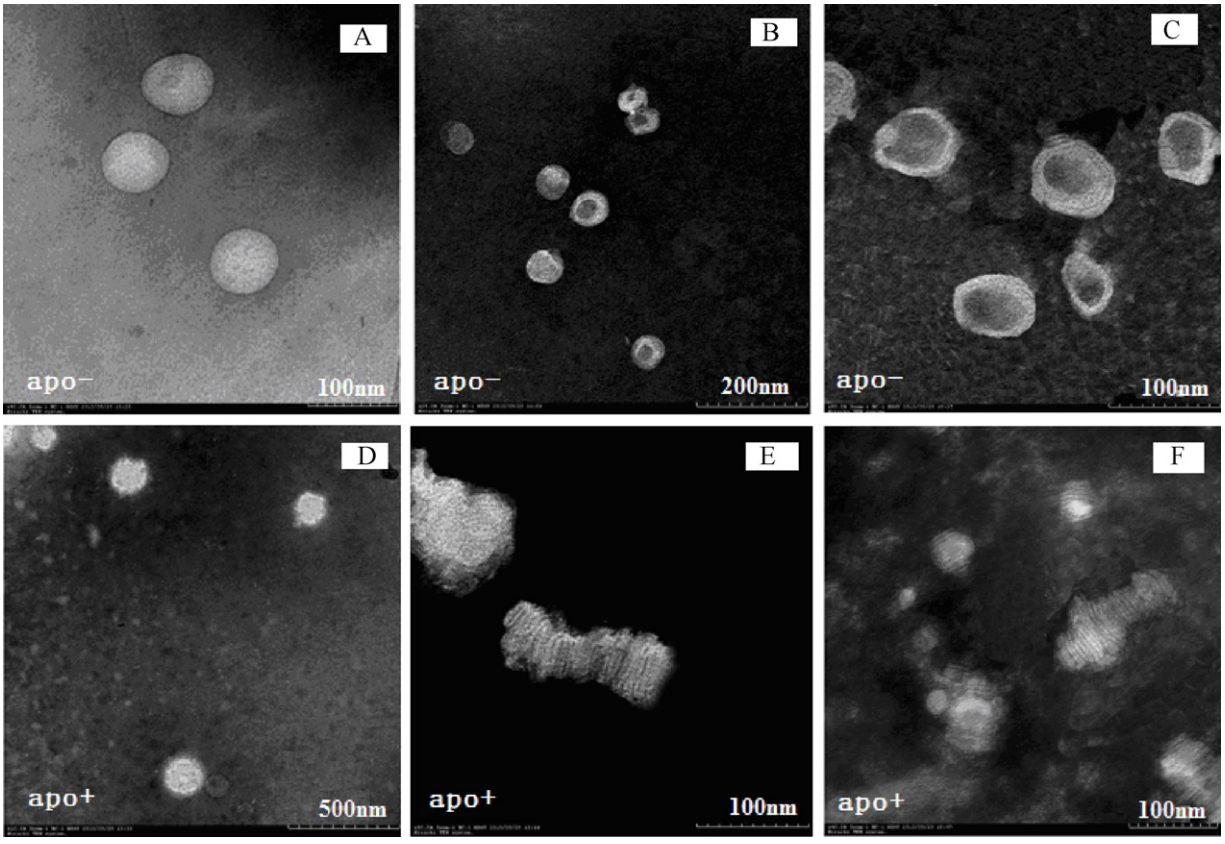

Fig. 1. Microphotographs of three TA-rHDL before (apo−) and after (apo+) incubation with apos by transmission electron microscope. (A) Lipid cores of TA-rHDL$_a$; (B) lipid cores of TA-rHDL$_b$; (C) lipid cores of TA-rHDL$_c$; (D) TA-rHDL$_a$; (E) TA-rHDL$_b$; (F) TA-rHDL$_c$.

Table 2
Fluorescence intensity of calcein in different TA-rHDL before and after incubation with apolipoproteins (mean ± SD, $n = 3$).

Formulation	Fluorescence intensity		Rate of change
	Before incubation	After incubation	
TA-rHDL$_a$	102.22 ± 3.49	111.19 ± 3.05	8.78 ± .0.03%
TA-rHDL$_b$	402.42 ± 6.35*	264.95 ± 5.20**	−34.16 ± 0.04%
TA-rHDL$_c$	476.35 ± 9.01**	243.95 ± 3.47*	−48.79 ± .0.03%

* Significant differences with TA-rHDL$_b$ vs TA-rHDL$_c$ in the same incubation state ($p < 0.05$).
** Significant differences with before vs after incubation in the same formulation ($p < 0.05$).

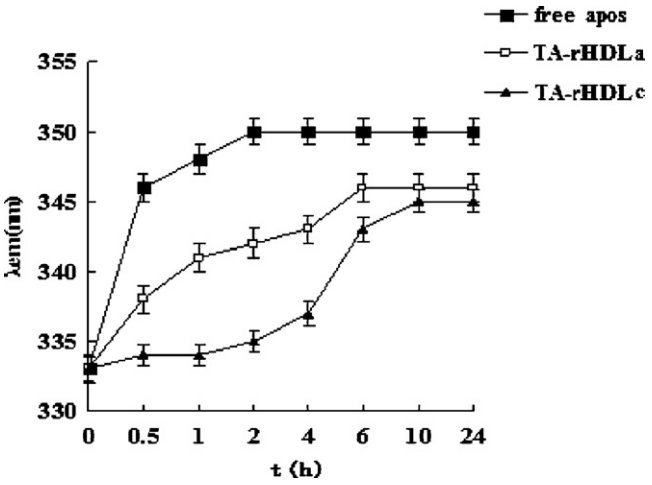

Fig. 2. Influence of GdnHCl on the fluorescence emission spectrum of apos free in solution and in the spherical and discoidal TA-rHDL.

was more significant. In addition, the calcein contents in TA-rHDL$_b$ (264.9) and TA-rHDL$_c$ (243.9) were virtually similar.

3.4. Guanidine hydrochloride denaturation experiments

Fig. 2 shows the fluorescence data of the apos denaturation by GdnHCl over 24 h. The maximal λ_{em} of apos either in free or lipid-bound form was close to 333 nm. The addition of GdnHCl resulted in apos denaturation with red shift of λ_{em}. Seen from the curves in Fig. 2, free apos were completely denatured by 2 M GdnHCl at 0.5 h, whereas the apos in the TA-rHDL presented slower increase of λ_{em} more significantly in the TA-rHDL$_c$ than in the TA-rHDL$_a$.

3.5. Phagocytosis tests

The results in Fig. 3 show that coupling apos with the lipid cores significantly increased the foam cell drug uptake for the spherical TA-rHDL irrespective of the VLDL in the culture medium (a vs b; c vs d). The presence of VLDL had significant influence on phagocytosis uptake of the spherical TA-rHDL by foam cells (b vs d). It was also noted that the uptake of TA-rHDL$_a$ without VLDL by foam cells was higher than that by macrophages (d vs e). In contrast, the drug uptake in the lipid cores by foam cells was weakened by VLDL in the medium (a vs c). Different from the spherical TA-rHDL$_a$, there was no further increase in TA-rHDL$_c$ uptake when VLDL were added (g vs h), however, boosted after exposure to LCAT (h vs i). Furthermore, the uptake of the discoidal TA-rHDL$_c$ by the foam cells was higher than that of TA-rHDL$_a$ at the same conditions (h vs b, g vs d). Also, the uptake of both spherical and discoidal TA-rHDL decreased with time of incubation.

The recombination behavior of structure of discoidal rHDL was further studied by fluorescent microscopic observations

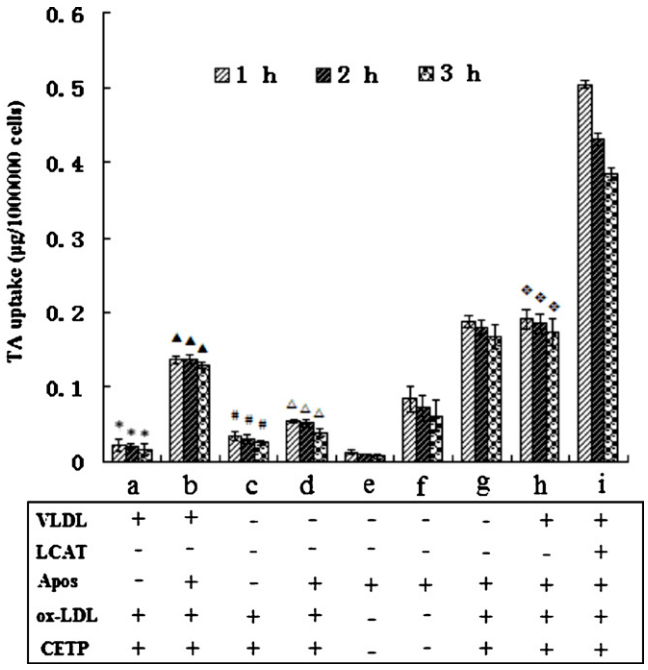

Fig. 3. Drug uptake of lipid cores of TA-rHDL$_a$ (a and c), TA-rHDL$_a$ (b, d and e) and TA-rHDL$_c$ (f–i) by macrophages (e and f) and foam cells expressing CETP (a–d and g–i) after different incubation periods. (a, b and h) In the presence of VLDL, (i) in the presence of VLDL and LCAT. Results (mean ± SD, $n = 3$) are expressed as the amount of TA phagocytozed with respect to 1,000,000 cells. Statistical significances ($p < 0.05$) between *: a and c; ▲: b and d; #: c and d; △: d and e; ❖: h and i. Table shows different conditions for phagocytosis test.

(Figs. 4 and 5). The green stains were foam cells which have phagocytosed fluorescent rHDL. In Fig. 4, rhodamine 123-labeled rHDL were phagocytosed even more actively when exposed to LCAT as revealed by the bright and diffuse pattern of fluorescence. On the contrary, calcein-labeled rHDL (Fig. 5) appeared to have less calcein phagocytosed after addition of LCAT.

4. Discussion

In this study, we prepared TA-loaded rHDL (TA-rHDL) with different structures and characterized from the standpoint of a new drug delivery system. We employed the rHDL as a targeting and functional carrier to deliver the cardiovascular drug.

The exact structure of TA-rHDL with different compositions was testified different from what is reported by other researchers (Feng et al., 2008a,b; Lou et al., 2005), possibly due to the discrepancies in drug polarity and content influencing the core structure. It was found that rHDL prepared with cholesteryl ester (CE) and glycerol trioleate (TG) were solid spheres, or else discs with a liposome-like structure. TA cannot substitute for CE to form the hydrophobic cores of rHDL, possibly loaded between lipid bilayers instead. This can be visualized by TEM photos and verified quantitatively by calcein tests. The low fluorescence intensity indicated little or no liposomal structures but rather a solid lipid sphere core existing in TA-rHDL$_a$. The slight increase for TA-rHDL$_a$ fluorescence intensities than their cores showed no differences ($p > 0.05$), which suggested high stability of TA-rHDL$_a$ core during the incubation process. The slight increase (8.7%) after incubation may be due to the adsorption of calcein to the amphiphilic apos. In contrast, the higher fluorescence intensities of the calcein in TA-rHDL$_b$ and TA-rHDL$_c$ implied the existence of liposomal cores in the formulations. In addition, leakage of calcein from TA-rHDL$_b$, particularly TA-rHDL$_c$, before and after incubation suggested that the change in the main liposomal vesicular structures in TA-rHDL$_b$ and TA-rHDL$_c$ had occurred

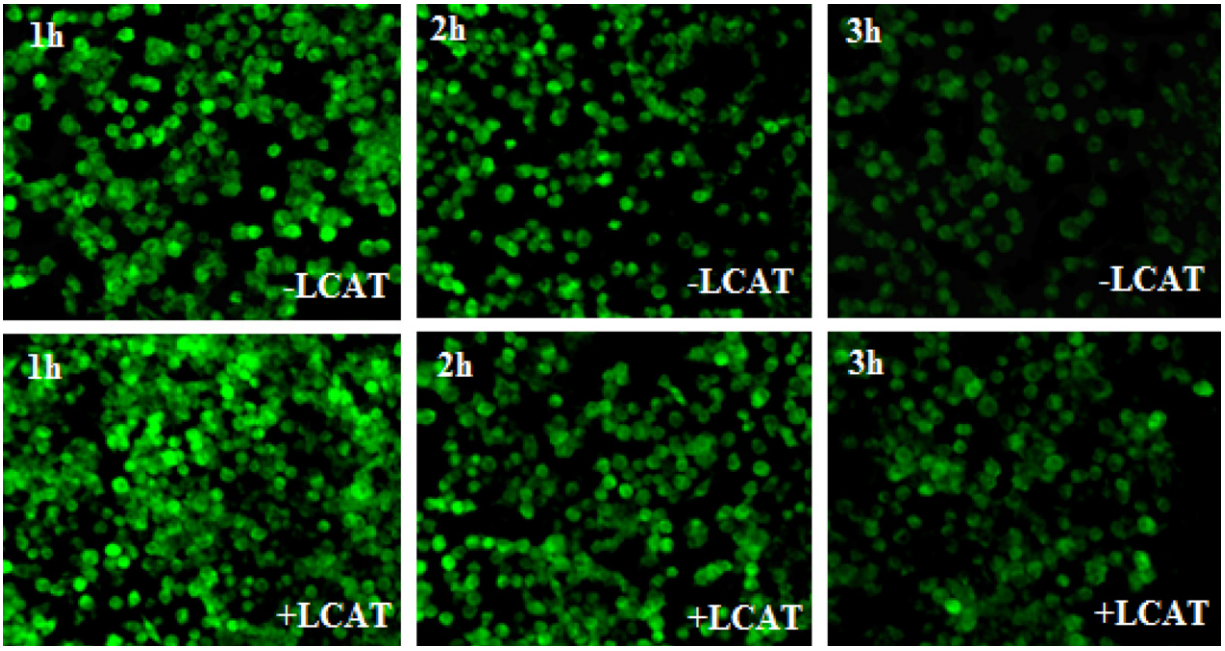

Fig. 4. Micrographs of foam cells after the uptake of rhodamin 123-labeled rHDL discs for 1 h, 2 h and 3 h incubation. Magnification: 10 × 10.

during coupling with apos. This may result from shrinked water cavities in TA-rHDL$_b$ and TA-rHDL$_c$ after incubation while converting from liposomes to discs (Fig. 1). The cores of TA-rHDL$_b$ and TA-rHDL$_c$ were prepared by two different methods. Their fluorescence intensities were different possibly due to their different entrapment efficiencies for calcein. However, the loss of calcein from TA-rHDL$_c$ and TA-rHDL$_b$ after incubation with apos suggested the resemblance in their internal structures.

The increase in particle size after incubation may result from a more hydrophilic surface (Ogino et al., 2010) and confirm the formation of a complex with the lipid core surrounded by the apos in the structure. The increase of the surface charge observed in TA-rHDL after incubation also indicated that apos, being amphipathic and negative-charged at pH 8.0, had been anchored on the surface of lipid cores.

In order to further ensure the formation of complex, stability of apos in free and lipid-bound forms was evaluated, respectively. The apos in the TA-rHDL presented an increased stability than free apos due to the presence of phospholipid (Reijngoud and Phillips, 1982; Sparks et al., 1992). It was convinced that the amphipathic α-helices of apos were embedded between phospholipid molecules with their hydrophobic faces in contact with phospholipid acyl chains (Segrest and Qarber, 1994) or presented in "double-belt" and/or "hairpin" model. Moreover, the different structural organizations of apoA-I on discoidal and spherical rHDL, as supported by fluorescence quenching results, led to different GdnHCl tolerances.

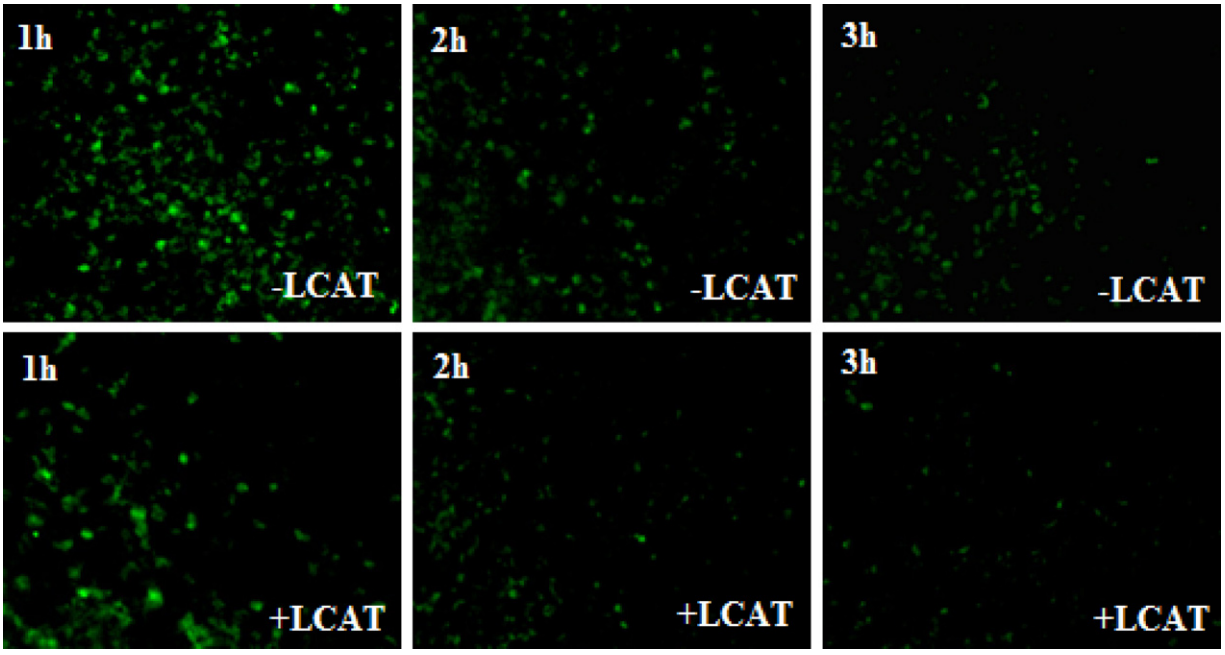

Fig. 5. Micrographs of foam cells after the uptake of calcein-labeled rHDL discs for 1 h, 2 h and 3 h incubation. Magnification: 10 × 10.

A major challenge we addressed in this study was to figure out the targeting mechanism to atherosclerotic plaque with TA-rHDL$_a$ and TA-rHDL$_c$ of different structures. There were probably two kinds of targeting mechanism. One was the direct apoA-I act on the receptors in the foam cells such as ABCA1 protein, ABCG-I and SR-BI (Collet et al., 1999; Fitzgerald et al., 2010; Hiltunen et al., 1998; Zannis et al., 2006), which was inferred from the significantly increased drug uptake of TA-rHDL$_a$ by foam cells after incubation with apos. The other was indirect targeting act through VLDL after structure remodeling of TA-rHDL. The presence of VLDL had remarkably increased uptake of TA-rHDL$_a$ by transfected foam cells expressing CETP, which implied that remodeling of spherical TA-rHDL may have contributed to specific targeting of TA-rHDL$_a$. During the remodeling process, TA-rHDL$_a$ may undergo a CE-TG interchange with VLDL under the action of CETP and lipase (Collet et al., 1999). Then the drug loaded in VLDL was taken up via the VLDL receptors by foam cells. It was reported that VLDL and SR-BI receptors in foam cells are related to cellular uptake of native HDL, SR-BI receptors for macrophages (Mahley and Innerarity, 1983). It was also noted that the uptake of TA-rHDL$_a$ without VLDL by foam cells was higher than that by macrophages (d vs e). This coincided with the findings (Hiltunen et al., 1998) that SR-BI and VLDL receptors in atherosclerotic lesions were both highly induced during cholesterol feeding to normal rabbits, and VLDL receptors upgraded faster initially. In contrast, the drug uptake in the lipid cores by foam cells was weakened by VLDL in the medium (a vs c), which may result from competitive effect of VLDL with their receptors.

Regarding discoidal TA-rHDL, two important conclusions may be drawn from aforementioned phenomena: (1) Discoidal TA-rHDL$_c$ may undergo a structure transformation from bilayer-discs to spheres, then deliver drug to foam cells in a similar pathway as TA-rHDL$_a$, which offered an explanation for the LCAT dependent increase of TA-rHDL$_c$ uptake. Furthermore, it can be concluded that the restructured TA-rHDL spheres from discs were more susceptible for internalization than artificial rHDL spheres (h vs b). (2) rHDL discs without VLDL and LCAT were speculated to be able to maintain the polar lipid bilayers, as in cell membranes (Phillips et al., 1997), therefore they were taken up more easily compared to TA-rHDL$_a$ (g vs d).

Also, the uptake of both spherical and discoidal TA-rHDL decreased with time of incubation. The likely explanation is that cells phagocytozing plenty of TA-rHDL had floated in the DMEM medium after 1 h and were washed away by D-PBS (Feng et al., 2005).

The opposite tendency in Figs. 4 and 5 for two florescent markers, one hydrophilic and one lipophilic, further proved the phenomenon of structure recombination from rHDL discs to spheres in the presence of LCAT (Pownall and Gotto, 1992). The remolding behavior of TA-rHDL discs were also observed by TEM (specific data will be reported in other paper). Since rHDL discs were composed of lipid bilayer, calcein can be loaded in aqueous cavity of rHDL and easily leaked out when rHDL recombined from discs to spheres, leading to decreased uptake when exposed to LCAT. In contrast, rhodamine 123 could still be entrapped in rHDL after structure change due to its high lipophilicity and affinity with the lipids, which was proved by enhanced uptake after exposure to LCAT.

5. Conclusions

The present work concerns the development of TA-rHDL to serve as a model to define structural feature and to explore the targeting mechanisms for atherosclerosis plaques. Specifically, the study investigated the new target pathways for atherosclerosis plaque of spherical and discoidal rHDL. The results showed that TA-rHDL prepared with CE and TG were spherical structure with increased stability of apos after lipid-binding. Phagocytosis studies showed both TA-rHDL discs and spheres had a target effect to foam cell through a receptor pathway associated the apos, and the uptake was enhanced by VLDL in the presence of CETP. Transformed TA-rHDL discs were taken up most actively when treated with LCAT.

In conclusion, TA-rHDL keeps discoidal and spherical shapes of native HDL and shows a preferential target for foam cell. These results might provide some helpful information to construct rHDL delivering lipophilic cardiovascular drug. Further studies are planned to investigate the size effect and *in vivo* targeting ability to atherosclerotic plaque, as well as the pharmacokinetics and pharmacodynamics of TA-rHDL.

Acknowledgements

This study is financially supported by the Major Project of National Science and Technology of China for New Drugs Development (No. 2009ZX09310-004) and the National Science Foundation Grant of China (No. 81072587). We thank Professor Hong-wen Zhou (Department of Endocrinology, Jiangsu Province Hospital) for his kind gift of CETP plasmid. We would like to acknowledge the invaluable assistance of Tonrol Bio-Pharmaceutical Co., Ltd. by providing raw material for isolation of apolipoproteins.

References

Ajees, A., Anantharamaiah, G., Mishra, V., Hussain, M., Murthy, H., 2006. Crystal structure of human apolipoprotein AI: insights into its protective effect against cardiovascular diseases. Proc. Natl. Acad. Sci. U.S.A. 103, 2126–2131.
Assmann, G., Nofer, J., 2003. Atheroprotective effects of high-density lipoproteins. Medicine 54, 321–341.
Barter, P., Nicholls, S., Rye, K., Anantharamaiah, G., Navab, M., Fogelman, A., 2004. Antiinflammatory properties of HDL. Circ. Res. 95, 764–772.
Bobryshev, Y., 2006. Monocyte recruitment and foam cell formation in atherosclerosis. Micron 37, 208–222.
Collet, X., Tall, A., Serajuddin, H., Guendouzi, K., Royer, L., Oliveira, H., Barbaras, R., Jiang, X., Francone, O., 1999. Remodeling of HDL by CETP in vivo and by CETP and hepatic lipase in vitro results in enhanced uptake of HDL CE by cells expressing scavenger receptor BI. J. Lipid Res. 40, 1185–1193.
Feng, M., Cai, Q., Huang, H., Zhou, P., 2008a. Liver targeting and anti-HBV activity of reconstituted HDL-acyclovir palmitate complex. Eur. J. Pharm. Biopharm. 68, 688–693.
Feng, M., Cai, Q., Shi, X., Huang, H., Zhou, P., Guo, X., 2008b. Recombinant high-density lipoprotein complex as a targeting system of nosiheptide to liver cells. J. Drug Target 16, 502–508.
Feng, M., Pan, S., Zhang, J., Wang, Q., Wu, W., Li, R., 2005. In vitro phagocytic uptake of PEG-PBLG nanoparticles containing amphotericin B. J. China Pharm. Univ. 36, 321–325.
Fitzgerald, M., Mujawar, Z., Tamehiro, N., 2010. ABC transporters, atherosclerosis and inflammation. Atherosclerosis 211, 361–370.
Fry, D., White, J., Goldman, I., 1978. Rapid separation of low molecular weight solutes from liposomes without dilution. Anal. Biochem. 90, 809–815.
Hiltunen, T., Luoma, J., Nikkari, T., Yla-Herttuala, S., 1998. Expression of LDL receptor, VLDL receptor, LDL receptor C related protein, and scavenger receptor in rabbit atherosclerotic lesions: marked induction of scavenger receptor and VLDL receptor expression during lesion development. Circulation 97, 1079–1086.
Jain, S., Chaurasiya, A., Gupta, Y., Jain, A., Dagur, P., Joshi, B., Katoch, V., 2008. Development and characterization of 5-FU bearing ferritin appended solid lipid nanoparticles for tumour targeting. J. Microencapsul. 25, 289–297.
Libby, P., Bonow, R., Mann, D., Zipes, D., 2008. Braunwald's Heart Disease: A Textbook of Cardiovascular Medicine, 8th ed. Saunders Elsevier, Philadelphia, PA.
Linsel-Nitschke, P., Tall, A., 2005. HDL as a target in the treatment of atherosclerotic cardiovascular disease. Nat. Rev. Drug Discov. 4, 193–205.
Lou, B., Liao, X., Wu, M., Cheng, P., Yin, C., Fei, Z., 2005. High-density lipoprotein as a potential carrier for delivery of a lipophilic antitumoral drug into hepatoma cells. World J. Gastroenterol. 11, 954–959.
Lusis, A., 2000. Athemsclerosis. Nature 407, 233–241.
Mahley, R., Innerarity, T., 1983. Lipoprotein receptors and cholesterol homeostasis. Biochim. Biophys. Acta 737, 197–222.
McConathy, W., Nair, M., Paranjape, S., Mooberry, L., Lacko, A., 2008. Evaluation of synthetic/reconstituted high-density lipoproteins as delivery vehicles for paclitaxel. Anticancer Drugs 19, 183–188.
Nanjee, M., Doran, J., Lerch, P., Miller, N., 1999. Acute effects of intravenous infusion of ApoA1/phosphatidylcholine discs on plasma lipoproteins in humans. Arterioscler. Thromb. Vasc. Biol. 19, 979–989.

Oda, M., Hargreaves, P., Beckstead, J., Redmond, K., van Antwerpen, R., Ryan, R., 2006. Reconstituted high density lipoprotein enriched with the polyene antibiotic amphotericin B. J. Lipid Res. 47, 260–267.

Ogino, C., Shibata, N., Sasai, R., Takaki, K., Miyachi, Y., Kuroda, S., Ninomiya, K., Shimizu, N., 2010. Construction of protein-modified TiO_2 nanoparticles for use with ultrasound irradiation in a novel cell-injuring method. Bioorg. Med. Chem. Lett. 20, 5320–5325.

Phillips, J., Wriggers, W., Li, Z., Jonas, A., Schulten, K., 1997. Predicting the structure of apolipoprotein AI in reconstituted high-density lipoprotein disks. Biophys. J. 73, 2337–2346.

Pownall, H., Gotto, A., 1992. Human plasma apolipoproteins in biology and medicine. Struct. Funct. Apolipoproteins, 1–32.

Reijngoud, D., Phillips, M., 1982. Mechanism of dissociation of human apolipoprotein AI from complexes with dimyristoylphosphatidylcholine as studied by guanidine hydrochloride denaturation. Biochemistry 21, 2969–2976.

Saito, H., Dhanasekaran, P., Nguyen, D., Deridder, E., Holvoet, P., Lund-Katz, S., Phillips, M., 2004. α-Helix formation is required for high affinity binding of human apolipoprotein AI to lipids. J. Biol. Chem. 279, 20974–20981.

Segrest, J., Qarber, D., 1994. The amphipathic a helix: a multifunctional structural motif in plasma apolipoproteins. Lipoproteins Apolipoproteins Lipases, 303–369.

Skajaa, T., Cormode, D., Jarzyna, P., Delshad, A., Blachford, C., Barazza, A., Fisher, E., Gordon, R., Fayad, Z., Mulder, W., 2010. The biological properties of iron oxide core high-density lipoprotein in experimental atherosclerosis. Biomaterials 32, 206–213.

Song, X., Fischer, P., Chen, X., Burton, C., Wang, J., 2009. An apoA-I mimetic peptide facilitates off-loading cholesterol from HDL to liver cells through scavenger receptor BI. Int. J. Biol. Sci. 5, 637–646.

Sparks, D., Lund-Katz, S., Phillips, M., 1992. The charge and structural stability of apolipoprotein AI in discoidal and spherical recombinant high density lipoprotein particles. J. Biol. Chem. 267, 25838–25839.

Thomas, M., Bhat, S., Sorci-Thomas, M., 2008. Three-dimensional models of HDL apoA-I: implications for its assembly and function. J. Lipid Res. 49, 1875–1883.

Vaisar, T., Pennathur, S., Green, P., Gharib, S., Hoofnagle, A., Cheung, M., Byun, J., Vuletic, S., Kassim, S., Singh, P., 2007. Shotgun proteomics implicates protease inhibition and complement activation in the antiinflammatory properties of HDL. J. Clin. Invest. 117, 746–756.

Viles-Gonzalez, J., Fuster, V., Corti, R., Badimon, J., 2003. Emerging importance of HDL cholesterol in developing high-risk coronary plaques in acute coronary syndromes. Curr. Opin. Cardiol. 18, 286–294.

Xie, S., Lee, Y., Kim, E., Chen, L., Ni, J., Fang, L., Liu, S., Lin, S., Abe, J., Berk, B., 2009. TR4 nuclear receptor functions as a fatty acid sensor to modulate CD36 expression and foam cell formation. Proc. Natl. Acad. Sci. U.S.A. 106, 13353–13358.

Zannis, V., Chroni, A., Krieger, M., 2006. Role of apoA-I, ABCA1, LCAT, and SR-BI in the biogenesis of HDL. J. Mol. Med. 84, 276–294.

Zhang, W., Gu, X., Bai, H., Yang, R., Dong, C., Liu, J., 2010. Nanostructured lipid carriers constituted from high-density lipoprotein components for delivery of a lipophilic cardiovascular drug. Int. J. Pharm. 391, 313–321.